Rare Metal Materials and Engineering
Volume 52, Issue 7, July 2023
Available online at www.rmme.ac.cn

Science Press

Cite this article as: Zhang Mingda, Shi Donggang, Hu Chundong, et al. Effect of Primary *α*-Phase on Micro-area Plastic Deformation of Ti6242s Alloy Under Dwell Fatigue[J]. Rare Metal Materials and Engineering, 2023, 52(07): 2317-2325.

ARTICLE

Effect of Primary α-Phase on Micro-area Plastic Deformation of Ti6242s Alloy Under Dwell Fatigue

Zhang Mingda[1], Shi Donggang[2], Hu Chundong[3], Cao Jingxia[1], Huang Hao[1], Huang Xu[1]

[1] Key Laboratory of Advanced Titanium Alloys, Beijing Institute of Aeronautical Materials, Aero Engine Corporation of China, Beijing 100095, China; [2] R&D Center, AECC Commercial Aircraft Engine Co., Ltd, Shanghai 201108, China; [3] School of Materials Science and Engineering, Shanghai University, Shanghai 200444, China

Abstract: The relationship between microstructure characteristics and fatigue properties of Ti-6Al-2Sn-4Zr-2Mo-0.1Si (Ti6242s) alloy was investigated. According to the microstructure quantitative analysis results, the solution treatments at different temperatures have an obvious effect on the proportion and morphology of primary *α*-phase. The changes in microstructure characteristics slightly influence the tensile property and low-cycle fatigue property of Ti6242s alloy at room temperature, whereas the dwell fatigue life and the fatigue sensitivity index are sensitive to these changes. Additionally, it is verified that the relatively strong stress concentration and inhomogeneous micro-area plastic deformation occur in the Ti6242s alloy under dwell fatigue load. Moreover, the characteristics of small plane regions and the surrounding quasi-cleavage regions in the Ti6242s alloy under dwell fatigue load at room temperature are formed through the analysis of fatigue failure fracture morphologies. The related experiment results are in good agreement with the stress-strain distribution characterizations of microstructures of equiaxed primary *α*-phase and the surrounding soft phase/grain. Accordingly, the relatively low inhomogeneous micro-area plastic deformation in the alloy with equiaxed primary *α*-phase of low volume fraction is beneficial to reduce the probability of crack initiation and can delay crack propagation, thus improving the dwell fatigue property.

Key words: titanium alloys; fatigue test; electron backscattered diffraction; micro-area plastic deformation; failure fracture analysis

Titanium alloy is an important lightweight metal material, which has been widely used in the aerospace, aviation, military, shipping, and energy industries. The high-temperature titanium alloys are mainly used to manufacture discs and blades in the fan and compressor sections of aero-engines. Several series of high-temperature titanium alloys have been developed for the manufacture of advanced aeroengines with higher, more diverse, and more complex performance requirements, such as IMI550, IMI685, IMI834, Ti17, and Ti-6Al-2Sn-4Zr-2Mo-0.1Si (Ti6242s) alloys. Ti6242s alloy is a typical high-temperature titanium alloy with high specific strength, excellent creep resistance, and good toughness, which usually serves at 500–550 °C. Similar to that of other near-α or $\alpha+\beta$ high-temperature titanium alloys, the dwell fatigue property of Ti6242s alloy requires thorough assessment before its application in aeroengines[1–2].

Dwell fatigue failure of near-α or $\alpha+\beta$ high-temperature titanium alloys differs from other conventional low-cycle and high-cycle fatigue failure modes. This premature fail behavior usually occurs under periodic dwell load. Since, the magnitude of dwell fatigue life of titanium alloys is increased with decreasing the temperature, this special failure mode is called as the cold-dwell fatigue. It is believed that many internal material factors[3–8], external testing, and environmental factors[9–13] can affect the cold-dwell fatigue property. Moreover, the cold-dwell fatigue failure of near-α or $\alpha+\beta$ titanium alloys is mainly related to the variety of alloys and the type of microstructures. The inhomogeneous plastic deformation and local stress concentration within the titanium alloy under dwell fatigue load are considered as the internal mechanism of the premature failure behavior[14–16]. The external test and environmental factors, including fatigue

Received date: October 08, 2022
Foundation item: National Natural Science Foundation of China (91860106)
Corresponding author: Hu Chundong, Ph. D., Associate Professor, School of Materials Science and Engineering, Shanghai University, Shanghai 200444, P. R. China, E-mail: hcd@shu.edu.cn

stress, stress ratio, temperature, waveform, and atmosphere, may enhance or weaken the dwell fatigue sensitivity of titanium alloy by affecting the internal mechanism. Hence, selecting an appropriate alloy or microstructure type is a simple but effective way to alleviate dwell fatigue. The dwell fatigue performance of different titanium alloys and microstructure types has been widely researched. Qiu et al[3] compared the dwell fatigue properties of Ti-6Al-2Sn-4Zr-*x*Mo (x=2 – 6) alloys based on the microstructure-normalized basis. It is found that with increasing the Mo content, the dwell fatigue life is rapidly reduced, and the dwell fatigue fractures appear on surface instead of subsurface. Zeng et al[7] discussed the influence of microstructures on dwell fatigue sensitivity of Ti-6.5Al-3.5Mo-1.5Zr-0.3Si alloy. Among the equiaxed, trimodal, and basketweave microstructures, the equiaxed microstructure has the strongest fatigue life reduction effect. Basketweave microstructure possesses a slightly higher dwell fatigue life, compared with that of tri-modal microstructure at low maximum stress. McBagonluri[4] and Shen[5] et al demonstrated that the equiaxed and elongated microstructures have shorter fatigue life and faster crack growth rate than the colony microstructure does. Woodfield et al[6] introduced the effect of microstructure on dwell fatigue behavior of β-heat-treated Ti6242 alloy. The neighboring primary α colony orientations possess important effects on the dwell fatigue crack initiation in a colony. Chandravanshi et al[14] found that the fine microstructures obtained by hot deformation usually have long fatigue life and long dwell fatigue life. The large reduction in $\alpha+\beta$ phase region can also be observed during the final hot deformation stages, which leads to the microstructure refinement and the formation of a large number of hard-orientated grains, thereby improving the dwell fatigue life. The effects of titanium alloys or their microstructure types on dwell fatigue property have been extensively researched. Usually, the low-cycle fatigue life and dwell fatigue properties of different titanium alloys with different microstructure types are quite different. Therefore, the preparation process need optimization.

This research investigated the effect of primary α-phase on the micro-area plastic deformation of Ti6242s alloy under low-cycle fatigue and dwell fatigue. Accordingly, the disc forgings of Ti6242s alloy with primary α-phase of different volume fractions and morphology characteristics were obtained via heat treatment at different temperatures. The microstructures of these forgings were observed and quantitatively analyzed. The mechanical properties, including tensile properties, low-cycle fatigue property, and dwell fatigue property at room temperature, were tested. The analysis of micro-area plastic deformation and failure fracture evaluation provided the effect mechanism of primary α-phase on dwell fatigue behavior of Ti6242s alloy.

1 Experiment

Four pieces of Ti6242s disc forgings were treated by solid solution at 970, 985, 995, and 1003 °C for 1 h, then aged at 595 °C for 8 h, and finally air cooled. Subsequently, the specimens for analysis of microstructure and mechanical properties were machined from the key center position of lengthwise section in these disc forgings, which were considered as the most sensitive position to dwell fatigue behavior in this research. The microstructures of Ti6242s alloy were then observed via optical microscope (OM, CARL ZEISS Axio Vert. A1) and scanning electron microscope (SEM, FEI Nova Nano SEM). The Kroll's reagent (2vol% HF and 10vol% HNO_3 in H_2O) was used to etch the specimens. The volume fraction and the average size of the equiaxed primary α-phase were measured. Every equiaxed primary α-grain could be identified by Image-Pro Plus analysis software. The volume fraction of the equiaxed primary α-phase was calculated by the ratio of the total area of the primary α-grain to the total measured area; the average grain size and average cross-section area of the primary α-phase were measured automatically according to the reference size. The tensile specimens and fatigue specimens were cut along the circumferential direction. The gage and grip diameters of the tensile specimen were 6 and 12 mm, respectively. The gage and grip diameters of the fatigue specimen were 6 and 14 mm, respectively. Room-temperature tensile tests were conducted according to ASTM-E8/E8M standard, and the room-temperature load-controlled fatigue tests were conducted according to ASTM-E466 standard. The low-cycle fatigue tests were conducted by triangular waveform with the maximum stress of 869 MPa and rise/down time of 1 s. The dwell fatigue tests were conducted by trapezoidal waveform with rise/down time of 1 s, and the dwell time was 120 s under the maximum stress of 869 MPa. The applied load was unidirectional tension, and the stress ratio of the low-cycle fatigue tests and dwell fatigue tests was 0. Three specimens for low-cycle fatigue tests and three specimens for dwell fatigue tests were tested until the fracture failure. Other fatigue specimens were tested after fatigue cycle of 200 times for the microstructure analysis. For microstructure analysis, the specimens were cut along the midline of the fatigue specimens. The electron backscattered diffractometer (EBSD) data were acquired by HKL Channel EBSD system, and the data were processed through Channel 5 software, presenting the grain boundary images and intragranular-local-misorientation maps. The analysis areas of the EBSD test were designed as 400 μm×300 μm, and the analysis step was 0.5 μm. Additionally, the intragranular-local-misorientation could be expressed by the kernel average misorientation (KAM) parameter. Therefore, KAM parameter was discussed. Afterwards, the average misorientation between the data point and its neighbors was calculated. The filter size of the intragranular-local-misorientation analysis in this study was 5×5. The characteristic morphologies of failure fracture in low-cycle fatigue specimens and dwell fatigue specimens were observed by SEM and analyzed.

2 Results and Discussion

2.1 Microstructure

Fig.1 shows OM original microstructures of Ti6242s alloys before fatigue tests. The microstructure consists of equiaxed primary α-phase (light phase) and transformed β-phase matrix

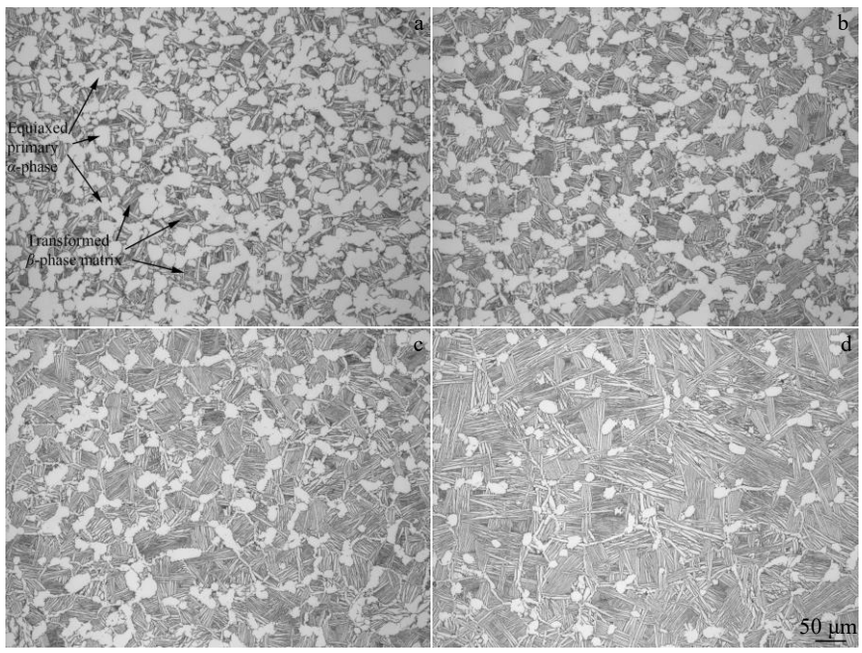

Fig.1 SEM original microstructures of Ti6242s alloys after solid-solution heat treatment at 970 °C (a), 985 °C (b), 995 °C (c), and 1003 °C (d)

(dark phase). The transformed β-phase matrix is composed of β colonies, and the α_s and β laths with the similar arraying directions in local areas are alternately arranged. It can be seen that the proportion of transformed β-phase matrix and the size of β colonies are increased with increasing the solution heat treatment temperature.

SEM microstructures of the transformed β-phase matrix are shown in Fig. 2. The size of α_s laths in the transformed β colonies is between 0.1 and 2.0 μm. Moreover, the β laths in the transformed β colonies are much thinner than those in the α_s laths. The heat treatment process has no obvious effect on the morphology of the transformed β-phase matrix, which is mainly due to the transformation of β-phase matrix during aging treatment at the same temperature. Both the equiaxed primary α-phase and α_s laths have close-packed hexagonal (hcp) crystal structure with strong anisotropy, whereas the β

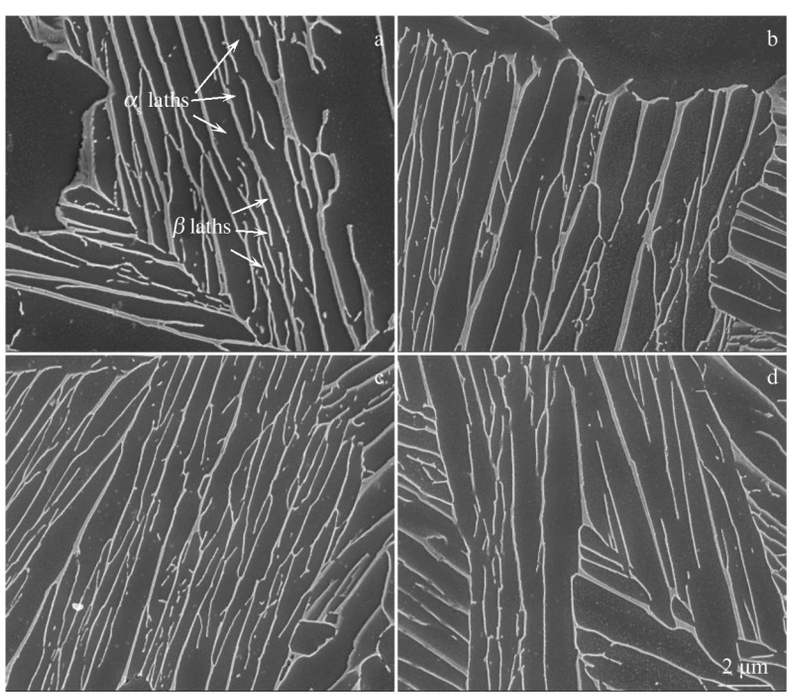

Fig.2 SEM microstructures of transformed β-phase matrix in Ti6242s alloys after solid-solution heat treatment at 970 °C (a), 985 °C (b), 995 °C (c), and 1003 °C (d)

laths in the transformed β colonies have body-centered cubic (bcc) crystal structure.

As shown in OM and SEM morphologies of Ti6242s alloy, different solution treatments mainly influence the microstructure characteristics of the primary α-phase, such as its proportion and morphology. The volume fraction, average grain size, and average sectional area of the primary α-phase are analyzed, as shown in Table 1. It can be seen that approximately 9.2vol% primary α-phase exists in the Ti6242s alloy after solution heat treatment at 1003 °C, and 37.1vol% primary α-phase exist in the alloy after solution heat treatment at 970 °C. Simultaneously, the distribution density, average grain size, and average sectional area of the primary α-phase are decreased with increasing the solution heat treatment temperature. At a certain temperature range below the $\alpha \leftrightarrow \beta$ phase transition temperature, the volume fraction of the primary α-phase is gradually decreased with increasing the solution temperature in traditional titanium alloy. In this research, the $\alpha \leftrightarrow \beta$ phase transformation temperature of Ti6242s alloy is between 1010 and 1015 °C, and the final forging temperature before heat treatment is lower than 970 °C. The solid solution process causes the phase transition from α-phase to β-phase, particularly at high solid solution temperatures, which results in the transformation from large primary α-grains into small primary α-grains. Some small primary α-grains even disappear completely. Therefore, the average primary α-grain size decreases, and the number of primary α-grains also reduces. In addition, the distribution of α-grains is dispersed and independent in the Ti6242s alloy after solid-solution heat treatment at 1003 °C.

Fig. 3 shows the contents of primary α-phase and the distribution of primary α-phase in the cross section of Ti6242s alloys after solid-solution heat treatment at different temperatures. The volume fraction of the primary α-phase is decreased with increasing the solution heat treatment temperature. The $\beta \rightarrow \alpha$ transition temperature of the Ti6242s alloy reaches nearly 1010 °C, as shown in Fig. 3a. When the solution heat treatment temperature approaches the phase transition temperature, the reduction in the volume fraction of primary α-phase becomes more obvious. Moreover, it can be seen that the area of primary α-phase in the cross section area is mainly 50–150 μm^2. Evidently, the solution heat treatment has a great influence on the content of primary α-phase, and the solution heat treatment at high temperatures results in the obvious reduction in primary α-grains.

2.2 Tensile and fatigue properties at room temperature

The tensile and fatigue tests were conducted at room temperature on the Ti6242s alloys after solid-solution heat treatment at different temperatures, and their results are shown in Fig. 4 and Fig. 5, respectively. The Ti6242s alloy has the ultimate tensile strength of 960–980 MPa, yield strength of 870–900 MPa, total elongation of 16%–21%, and the area reduction of 32% – 39%. The ultimate tensile strength is increased slightly, whereas the yield strength, the total elongation, and the area reduction are decreased slightly with increasing the solution heat treatment temperature. In conclusion, the microstructure characteristics present the marginal effect on tensile property and low-cycle fatigue property at room temperature.

The average cycle number of low-cycle fatigue test of different Ti6242s alloys is 12 000–18 000, demonstrating no significant correlation between the low-cycle fatigue property

Table 1 Analysis results of primary α-phase in Ti6242s alloy specimens after solid-solution heat treatment at different temperatures

Specimen	Heat treatment	Volume fraction/vol%	Distribution density/mm^{-2}	Average grain size/μm	Average sectional area/μm^2
1#	970 °C/1 h+595 °C/8 h	37.1	1219	16.95	317.78
2#	985 °C/1 h+595 °C/8 h	28.2	1041	16.44	283.08
3#	995 °C/1 h+595 °C/8 h	19.1	931	15.00	214.31
4#	1003 °C/1 h+595 °C/8 h	9.2	520	14.19	184.59

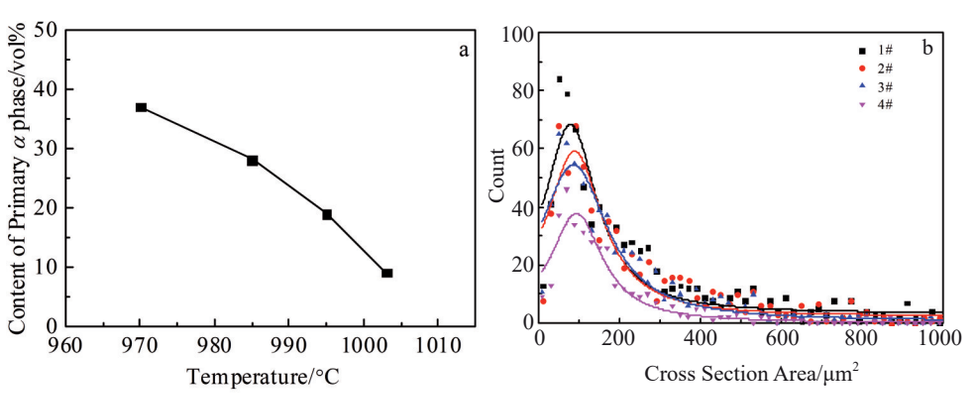

Fig.3 Contents of primary α-phase (a) and distribution of primary α-phase in cross section (b) of Ti6242s alloys after solid-solution heat treatment at different temperatures

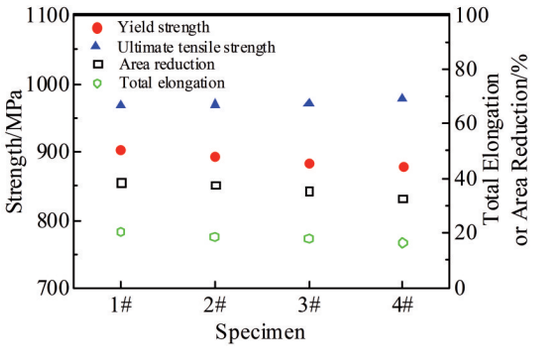

Fig.4 Room-temperature tensile properties of Ti6242s alloys after solid-solution heat treatment at different temperatures

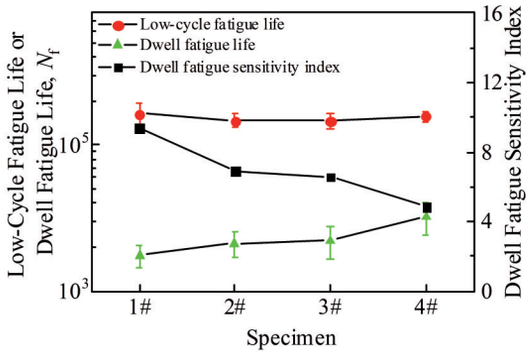

Fig.5 Room-temperature low-cycle fatigue life, dwell fatigue life, and dwell fatigue sensitivity index of Ti6242s alloys after solid-solution heat treatment at different temperatures

and the microstructure characteristics. However, the average failure cycle number of dwell fatigue test is increased from 1750 to 3250 with increasing the solid-solution heat treatment temperature. Accordingly, the fatigue sensitivity index and the ratio of low-cycle fatigue failure cycle to the dwell fatigue failure cycle are decreased with increasing the solution heat treatment temperature. Furthermore, the regular changes in dwell fatigue life confirm that the dwell fatigue performance of titanium alloy is sensitive to the characteristics of microstructures, as shown in Fig.5.

2.3 Microstructure evolution after dwell fatigue load

Dwell fatigue load at room temperature has no obvious effect on the morphology characteristics of the equiaxed primary α-phase and transformed β-phase matrix. However, according to the corrosion features under the same corrosion conditions, the stress concentration may occur in the phase interface between the equiaxed primary α-phase and transformed β-phase, as shown in Fig. 6. The stress usually accelerates the corrosion of metallic materials[17–18]. The internal stress in the material can also cause the difference in corrosion degree of microstructures. Many gullies and pits forming at the phase interface can be observed during the corrosion process, and the more the equiaxed primary α-phase, the easier the cessation occurrence in the specimens.

The stress concentration and inhomogeneous micro-area plastic deformation have been validated in the intragranular-local-misorientation analysis. Fig. 7 shows the intragranular-local-misorientation maps of Ti6242s alloys after solid-solution heat treatment at different temperatures followed by dwell fatigue of 200 cycles. The intragranular-local-misorientation is expressed by KAM in EBSD analysis, which usually represents the plastic strain level in the local area. In this research, the angle range of the intragranular-local-misorientation is defined as 0°–3°, and the intragranular-local-misorientation is inhomogeneously distributed in local areas. The high intragranular-local-misorientation areas are mainly concentrated in the transformed β colonies and some equiaxed primary α-grains, whereas the low intragranular-local-misorientation areas consisting of equiaxed primary α-grains exist as isolated islands. The inhomogeneous degree of intragranular-local-misorientation is equivalent to the inhomogeneous plastic deformation in the local area. According to Fig.7, the great deformation degree and the large difference in micro-area plastic deformation behavior can be observed in the Ti6242s alloy with the primary α-phase of high contents.

Fig. 8 provides the distributions of KAM parameters of the

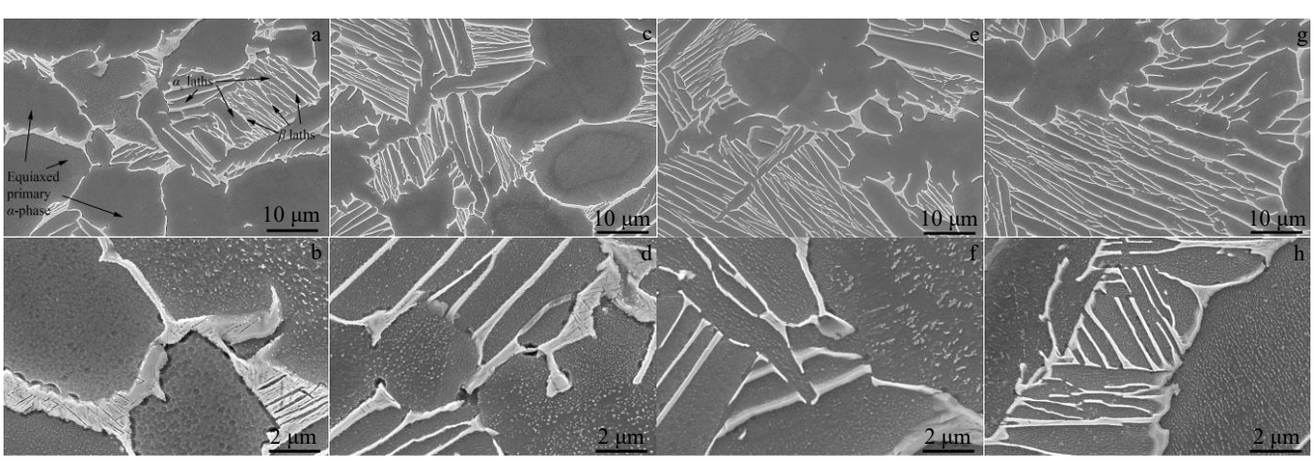

Fig.6 SEM microstructures of Ti6242s alloys after solid-solution heat treatment at 970 °C (a–b), 985 °C (c–d), 995 °C (e–f), and 1003 °C (g–h) followed by dwell fatigue of 200 cycles

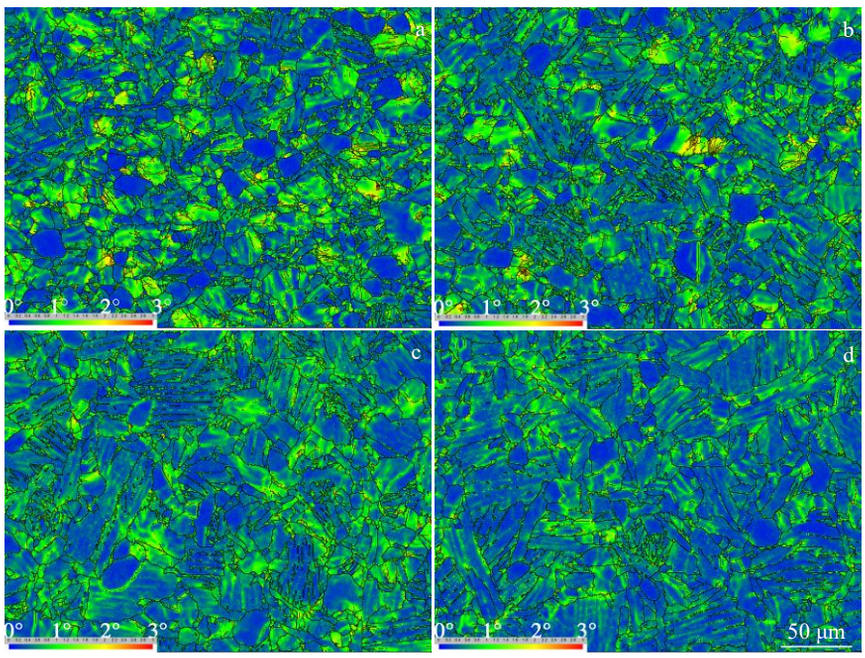

Fig.7 Intragranular-local-misorientation maps of Ti6242s alloys after solid-solution heat treatment at 970 °C (a), 985 °C (b), 995 °C (c), and 1003 °C (d) followed by dwell fatigue of 200 cycles

primary α-phase and transformed β-phase in Ti6242s alloys after solid-solution heat treatment at different temperatures followed by dwell fatigue of 200 cycles. The peak position of β-phase misorientation is at approximately 0.75°, which is higher than that of the primary α-phase (0.5°), indicating that the β-phase is prone to plastic deformation, compared with the primary α-phase in the Ti6242s alloy. The large amount of low KAM misorientation demonstrates that the micro-area plastic deformation of the microstructure obtained via high-temperature solution treatment is relatively lower and more uniform.

The inhomogeneous plastic deformation behavior of the Ti6242s alloy under dwell fatigue load can also be reflected by the fatigue failure fracture morphologies. The low-cycle fatigue load at room temperature can cause crack initiation failure on the surface of Ti6242s alloy specimens, as shown in Fig. 9. The characteristics of crack initiation source, fatigue strip, and transient fracture dimple can be easily identified. A completely different failure mode occurs in the Ti6242 alloy under dwell fatigue load at room temperature, as shown in Fig. 10. The dwell fatigue failure fractures present the internal crack initiation. A large number of fracture source characteristics can be observed in the inner area of fracture, presenting numerous bright white spots. Moreover, these internal crack source areas are composed of a small plane region and surrounding quasi-cleavage regions, as shown in Fig. 10. The central small plane region is flat and smooth, and its size is similar to that of the primary α-grain. Meanwhile, the small plane region is approximately perpendicular to the applied load direction. Furthermore, the quasi-cleavage regions originating from the central small plane region gradually expand to the dimple tearing region, and the quasi-cleavage expansion region also has the small stepped regions of different angles.

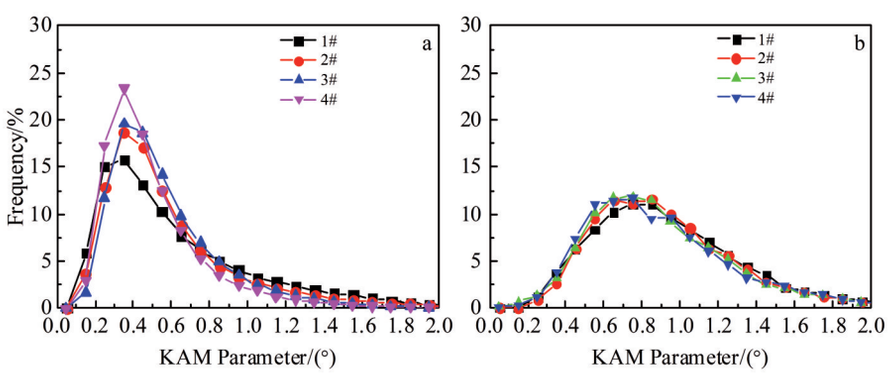

Fig.8 KAM parameter distributions of hcp primary α-phase (a) and bcc β-phase (b) in Ti6242s alloys after solid-solution heat treatment at different temperatures followed by dwell fatigue of 200 cycles

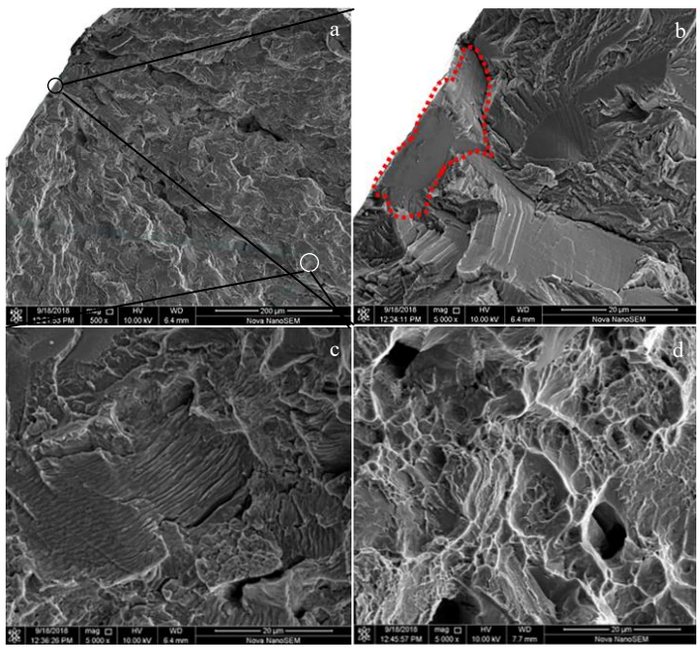

Fig.9 Fracture morphologies of Ti6242s alloys after low-cycle fatigue load of 869 MPa: (a) overall fracture morphology; (b) crack initiation source; (c) fatigue strip; (d) transient fracture dimple

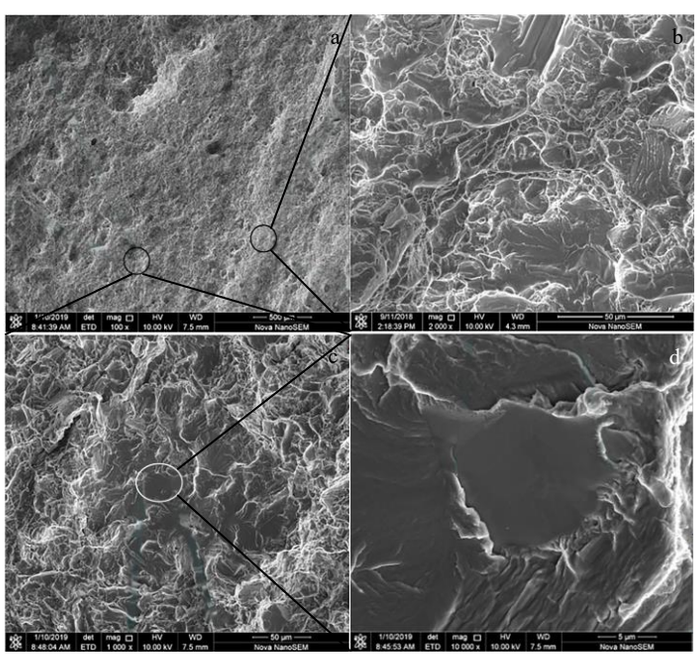

Fig.10 Fracture morphologies of Ti6242s alloys after dwell fatigue load of 869 MPa at room temperature: (a) overall fracture morphology; (b) transient fracture dimple; (c) internal crack initiation source+surrounding quasi-cleavage region; (d) internal crack initiation source

According to the inhomogeneous plastic deformation at the local area in EBSD test and the central small plane region surrounded by the quasi-cleavage regions in the fracture test, the dwell fatigue failure mechanism is closely related to the microstructure of Ti6242s alloy. During the dwell fatigue test, different levels of micro-area plastic deformation occur in the Ti6242s alloy, and a small number of equiaxed α-phase grains are not prone to deformation. The difference in micro-area plastic deformation between these hard-to-be-deformed equiaxed α-phase grains and the surrounding easy-to-be-deformed microstructure gradually accumulates under the dwell fatigue load. Moreover, the internal stress between them initially breaks the equiaxed α-phase grain, forming the small plane regions. Then, the crack source gradually grows to the surrounding transformed β-phase matrix under periodic loads, forming the quasi-cleavage regions of the crack morphology. More cracks are continuously formed, propagated, and merged, eventually leading to the failure and fracture of

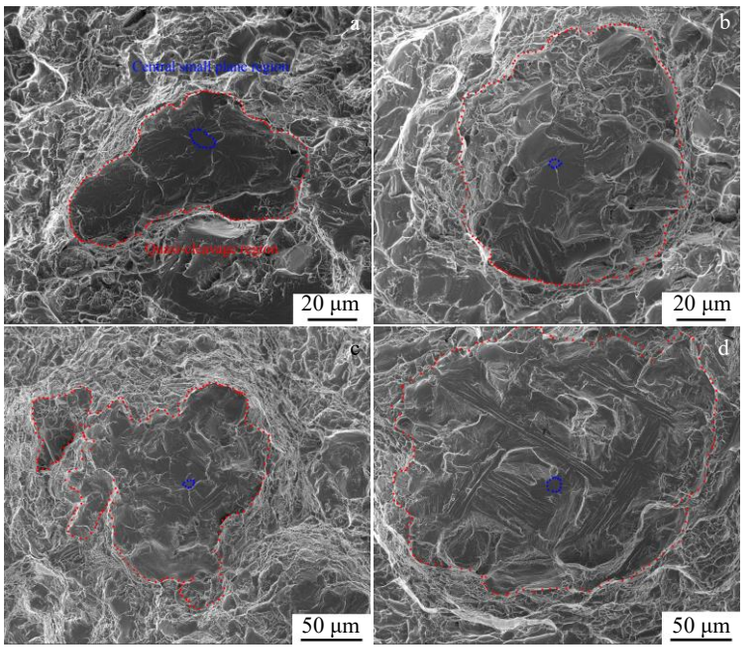

Fig.11 Fracture morphologies of Ti6242s alloys after solid-solution heat treatment at 970 °C (a), 985 °C (b), 995 °C (c), and 1003 °C (d) followed by dwell fatigue

Ti6242s alloys. These results are all related to the hard-orientated equiaxed primary α-phase with low plastic deformation and soft phase/grain with high plastic deformation.

The fracture morphologies of Ti6242s alloys after solid-solution heat treatment at different temperatures followed by dwell fatigue treatment are shown in Fig.11. The areas of the central small plane region range from tens of square microns to nearly one hundred square microns, which overlaps with the area of the equiaxed primary α -phase. No obvious difference in the small plane regions of the Ti6242s alloy with different microstructures can be observed. The areas of quasi-cleavage regions are between thousands of square microns and tens of thousands of square microns, which are ten times larger than those of the small plane regions. The relatively large quasi-cleavage areas can be observed after solution heat treatments at high temperatures. Additionally, the alloys after solution heat treatment at high temperatures have relatively low inhomogeneous plastic deformation degree at the local area, which reduces the probability of crack initiation. Furthermore, the β-phase matrix of high volume fraction increases the difficulty in crack propagation and reduces the probability of crack combination, thus improving the fatigue life of the Ti6242s alloy under dwell fatigue load.

3 Conclusions

1) The solution treatment process mainly changes the volume fraction, distribution density, average grain size, and average sectional area of the primary α-phase in the Ti-6Al-2Sn-4Zr-2Mo-0.1Si (Ti6242s) alloys. These microstructure characteristics present the marginal effect on tensile property and low-cycle fatigue property at room temperature. Meanwhile, the dwell fatigue life and the fatigue sensitivity index are highly sensitive to the microstructure characteristics, which are increased and decreased with increasing the solution treatment temperature, respectively.

2) The stress concentration and inhomogeneous micro-area plastic deformation are formed dramatically in the Ti6242s alloy under dwell fatigue load. The great deformation degree and the large difference in micro-area plastic deformation behavior can be observed in the Ti6242s alloy with the primary α-phase of high contents.

3) The inhomogeneous micro-area plastic deformation occurs in the Ti6242s alloys during fatigue failure fracture. The entirely different mode of internal crack initiation failure causes the small plane region and the surrounding quasi-cleavage regions in the Ti6242s alloy under dwell fatigue load at room temperature. This phenomenon is related to the hard equiaxed primary α -grains with low plastic deformation ability and nearby soft phase/grain with high plastic deformation ability.

4) The relatively low difference in inhomogeneous plastic deformation degree at the local area reduces the probability of crack initiation and hinders the crack propagation in the Ti6242s alloy with equiaxed primary α-phase of low content, thereby improving the fatigue property of the Ti6242s alloy under dwell fatigue load.

References

1 Shi Donggang, Xu Xiaoyan, Wu Yu *et al*. *Materials China*[J], 2019, 38(7): 722 (in Chinese)

2 Bache M R. *International Journal of Fatigue*[J], 2003, 25: 1079

3 Qiu J K, Ma Y J, Lei J F *et al*. *Metallurgical and Materials Transactions A*[J], 2014, 45(13): 6075

4 McBagonluri F, Akpan E, Mercer C *et al*. *Materials Science and Engineering A*[J], 2005, 405(1–2): 111
5 Shen W, Soboyejo W O, Soboyejo A B O. *Mechanics of Materials*[J], 2004, 36(1–2): 117
6 Woodfield A P, Gorman M D, Sutliff J A *et al*. *TMS Fall Meeting 98: Symposium on Fatigue Behavior of Titanium Alloys*[C]. Chicago: TMS, 1998
7 Zeng W D, Zhou Y G. *Materials Science and Engineering A*[J], 2000, 290(1–2): 33
8 Xi G Q, Lei J F, Qiu J K *et al*. *Materials and Design*[J], 2020, 194: 108 909
9 Fernandes M F, De Oliveira Velloso V M, Voorwald H J C. *Procedia Structural Integrity*[J], 2022, 35: 141
10 Tympel P O, Lindley T C, Saunders E A *et al*. *Acta Materialia*[J], 2016, 103: 77
11 Evans W J, Gostelow C R. *Metallurgical Transactions A*[J], 1979, 10(12): 1837
12 Gerland M, Lefranc P, Doquet V *et al*. *Materials Science and Engineering A*[J], 2009, 507(1–2): 132
13 Guo Ping, Pan Hao, Jia Guouy *et al*. *Rare Metal Materials and Engineering*[J], 2022, 51(1): 301 (in Chinese)
14 Chandravanshi V, Prasad K, Singh V *et al*. *International Journal of Fatigue*[J], 2016, 91: 100
15 Shen W, Soboyejo A B O, Soboyejo W O. *Symposium on Fatigue*[C]. Seattle: ASTM, 2002: 227
16 Wang X, Jahazi P V M, Yue S. *Metallurgical and Materials Transactions A*[J], 2007, 38(4): 831
17 Lv Y T, Ding Y, Cui H Z *et al*. *Materials Characterization*[J], 2020, 164: 110 351
18 Ning Z Y, Zhou Q L, Liu Z H *et al*. *Corrosion Science*[J], 2021, 189: 109 595

初生*α*相对Ti6242s合金在保载疲劳载荷作用下微区塑性变形的影响

张明达[1]，史栋刚[2]，胡春东[3]，曹京霞[1]，黄　浩[1]，黄　旭[1]
(1. 中国航空发动机集团 北京航空材料研究院 先进钛合金重点实验室，北京 100095)
(2. 中国航空发动机集团商用飞机发动机有限公司 研发中心，上海 201108)
(3. 上海大学 材料科学与工程学院，上海 200444)

摘　要：分析Ti-6Al-2Sn-4Zr-2Mo-0.1Si（Ti6242s）合金的组织特征和疲劳性能的关系。微观组织定量分析结果显示，不同温度固溶处理对初生*α*相的比例和形貌有明显影响，这些微观结构特征的变化对Ti6242s合金的室温拉伸性能和低周期疲劳性能有轻微的影响，但是对室温保载疲劳和保载疲劳敏感性有明显影响。随后分析证实了Ti6242s合金在保载疲劳载荷作用下存在相对较强的应力集中和不均匀微区塑性变形情况。而且，通过对疲劳失效断口形貌分析也证实了Ti6242s合金在室温保载疲劳下形成小平面特征和附近的准解理断裂区域特征，相关测试结果恰好对应等轴初生*α*相和附近的软相/软晶粒的微观组织应力应变分布表征结果。因此，在具有较低体积分数等轴初生*α*相的合金中形成相对较低程度的微区不均匀塑性变形，有助于降低裂纹萌生的概率并延迟裂纹扩展，从而改善保载疲劳性能。

关键词：钛合金；疲劳测试；背散射电子衍射；微区塑性变形；失效断口分析

作者简介：张明达，男，1987年生，博士，高级工程师，中国航空发动机集团北京航空材料研究院先进钛合金重点实验室，北京 100095，E-mail：mingda.zhang@biam.ac.cn